Chemistry A European Journal

Chemistry Europe
European Chemical Societies Publishing

Accepted Article

Title: In situ Mass Spectrometric and Kinetic Investigations of Soai's Asymmetric Autocatalysis

Authors: Oliver Trapp, Saskia Lamour, Frank Maier, Alexander Siegle, Kerstin Zawatzky, and Bernd F. Straub

To be cited as: *Chem. Eur. J.* 10.1002/chem.202003260

Link to VoR: https://doi.org/10.1002/chem.202003260

WILEY-VCH

WILEY-VCH

Research Article

In situ Mass Spectrometric and Kinetic Investigations of Soai's Asymmetric Autocatalysis

Oliver Trapp,*[a,b] Saskia Lamour,[a,b] Frank Maier,[a] Alexander F. Siegle,[a] Kerstin Zawatzky,[a] and Bernd F. Straub[c]

Abstract: *Chemical reactions that lead to a spontaneous symmetry breaking or amplification of the enantiomeric excess are of fundamental interest in explaining the formation of a homochiral world. An outstanding example is Soai's asymmetric autocatalysis, in which small enantiomeric excesses of the added product alcohol are amplified in the reaction of diisopropylzinc and pyrimidine-5-carbaldehydes. The exact mechanism is still in dispute due to complex reaction equilibria and elusive intermediates. In situ high-resolution mass spectrometric measurements, detailed kinetic analyses and doping with in situ reacting reaction mixtures, show the transient formation of hemiacetal complexes, which can establish an autocatalytic cycle. We propose a mechanism that explains the autocatalytic amplification involving these hemiacetal complexes. Comprehensive kinetic experiments and modelling of the hemiacetal formation and the Soai reaction allow the precise prediction of the reaction progress, the enantiomeric excess as well as the enantiomeric excess dependent time shift in the induction period. Experimental structural data give insights into the privileged properties of the pyrimidyl units and the formation of diastereomeric structures leading to an efficient amplification of even minimal enantiomeric excesses, respectively.*

Autocatalysis and in particular self-amplifying chemical processes are of great interest as they provide an explanation for the efficient replication of molecules with intrinsic error correction in general,[1] and the appearance of mirror image molecules with the same handedness, namely homochirality. Such processes are of fundamental importance in symmetry breaking[2] related to the emergence of life.[3] In an asymmetric reaction or catalysis, it is usually expected that the enantiomeric excess of the reagent or catalyst used will be transferred linearly to the product formation. Positive nonlinear effects,[4] which means that the use of only enantiomerically enriched reagents or catalysts lead to a significant increase in the enantiomeric excess in the product, are rarely observed. Mechanistic explanations for such reactions with positive nonlinear effects were discussed by Kagan[5] and Noyori.[6,7] considering reversible monomer-dimer associations. Frank[8] postulated a theoretical model leading to a spontaneous asymmetric synthesis. If dimers can be formed from their monomeric building blocks, e.g. by intermolecular interactions, they are of the same configuration (homochiral) or of opposite configuration (heterochiral). Since these homochiral and heterochiral dimers are diastereomeric to each other, they have different intrinsic properties, which are reflected in their solubility, rate of formation and other physical properties. The formation of heterochiral dimers from an enantiomerically enriched mixture can increase the enantiomeric excess of the free monomeric major enantiomer.[9]

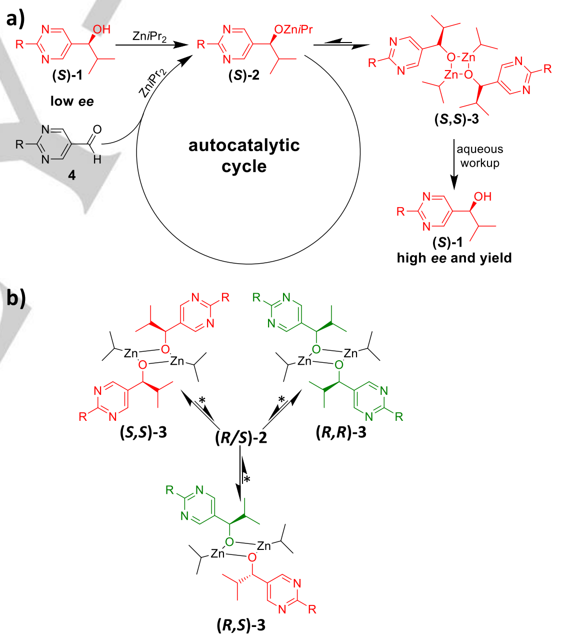

Scheme 1. Soai's asymmetric autocatalytic reaction. a) Conversion of pyrimidine-5-carbaldehyde **4** with diisopropylzinc (iPr_2Zn) in the presence of a catalytic amount of pyrimidyl alcohol **1**. b) Formation of homochiral **(*R*,*R*)-3**/ **(*S*,*S*)-3** and heterochiral **(*R*,*S*)-3** dimers of the isopropylzinc pyrimidyl alkoxides **2**. *The dimers can exchange their monomeric moieties without formation of the monomers **2**.[32] R = $(H_3C)_3C$-C≡C-.

In 1995, Soai[10,11] reported an extremely remarkable reaction. When pyrimidine-5-carbaldehyde **4** reacts with diisopropylzinc (iPr_2Zn) in the presence of a catalytic amount of pyrimidyl alcohol **1** with a low *ee*, asymmetric autocatalytic amplification of the enantiomeric excess gives the pyrimidine alcohol **1** with high *ee* as the final product (Scheme 1a). Autocatalysis and amplification are also observed in pyridyl-3-carbaldehydes,[12] however the 2-alkynyl substituted pyrimidine analogues are superior in amplification of the *ee*. Even a trace imbalance of chiral molecules[13] such as an extremely low *ee* of

[a] Prof. Dr. O. Trapp, Dr. S. Lamour, Dr. F. Maier, Dr. A.F. Siegle, Dr. K. Zawatzky
Department of Chemistry
Ludwig-Maximilians-University Munich
Butenandtstr. 5-13
81377 Munich (Germany)
E-mail: oliver.trapp@cup.uni-muenchen.de

[b] Max-Planck-Institute for Astronomy
Königstuhl 17
69117 Heidelberg (Germany)

[c] Prof. Dr. B.F. Straub
Organisch-Chemisches Institut
Ruprecht-Karls-Universität Heidelberg
Im Neuenheimer Feld 270
69120 Heidelberg (Germany)

Supporting information for this article is given via a link at the end of the document the initial catalyst of only ~5·10^{-5} %[14] or other chiral triggers like $^{1}H/^{2}H$,[15] $^{12}C/^{13}C$,[16] $^{14}N/^{15}N$[17] and $^{16}O/^{18}O$[18] isotopically labelled cryptochiral compounds,[19] cryptochiral compounds,[20] circularly polarized light,[21] (enantiomorph) crystals[22] and other compounds[23] are able to induce enantioselectivities, that lead to an amplification greater than 99.5% *ee* in a few cycles. A highly interesting feature of the reaction is, that spontaneous symmetry breaking with stochastic distribution of the final **(*R*)-1** or **(*S*)-1** product is possible, even when no chiral additive is employed.[24]

Numerous findings and reports contributed to the mechanistic understanding of the Soai reaction.[2] Still, open questions remain, especially regarding (a) the origin of enantioselectivity, (b) kinetic aspects of the reaction, i.e. the reliable prediction of the chiral amplification, and (c) the privileged structure of the pyrimidyl-5-carbaldehydes and corresponding alcohols. While the last point (c) can be explained by experimental findings of similar reactions with the possible coordination of the nitrogen containing pyridyl or pyrimidyl rings and the associated activation of the alkyl zinc compounds as well as the formation of supramolecular structures,[6a] points a) and b) are not that obvious. The elucidation of the mechanism is highly challenging due to complex reaction equilibria and elusive intermediates.[25-29] It is well established that isopropylzinc pyrimidyl alkoxides **2** can form dimers, tetramers[30,31] and oligomeric compounds.[2] The dimers can be either homochiral (**(*R*,*R*)-3** or **(*S*,*S*)-3**) or heterochiral (**(*R*,*S*)-3**) (Scheme 1b).[32] It is important to note, that the interconversion of the dimers **3** can proceed by direct exchange of the monomeric moieties without formation of the monomers.[32] The implication of this equilibrium is, that the equilibrium constant for the heterochiral dimer formation K_{hetero} is twice the equilibrium constant for the homochiral dimer formation $K_{\text{hetero}}/K_{\text{homo}} = 2$.[33] Thus, nonlinear effect can be well explained, because an imbalance of the enantiomers leads to amplification as soon as more stable heterochiral dimers **(*R*,*S*)-3** have formed. Blackmond and Brown developed a model considering dimers **3** as catalytically active species based on reaction progress analysis by calorimetric measurements and NMR spectroscopy. These dimers, tetramers[30,31] and oligomers[34] were characterized by comprehensive NMR spectroscopic measurements and single-crystal X-ray diffraction analysis,[35] and these findings are supported by quantum chemical computations.[36] Kinetic studies corroborate these results with pronounced effects of the additive concentration[37] and *ee* leading to an induction period and a sigmoidal kinetic profile typical for autocatalytic processes.[2] Schiaffino performed quantum chemical calculations of the kinetic constants at the M05-2X/6-31G(d) level of theory and investigated the effect of the aza group in the pyrimidine moiety to activate the zinc reagent in the tetrameric complex.[38]

In 2012 Brown, Blackmond and co-workers[39] reported the identification of a transient hemiacetal intermediate in the Soai reaction of 2-(adamantylacetylene-1-yl)pyrimidine-5-carbaldehyde and 2-(adamantylacetylene-1-yl)pyrimidyl alcohol by ^{1}H NMR spectroscopic kinetic studies. Gridnev and Vorobiev investigated by quantum chemical DFT calculations and kinetic analysis potential acetal intermediates. They concluded that the acetals are off-loop species because they are not precursor of the reaction product.[27]

In this context, another highly remarkable discovery was reported by Hawbaker and Blackmond, where hydroxy ethers interfere with the Soai reaction and even inhibit the reaction.[19]

More recently, Denmark and co-workers[40] performed investigations of the Soai reaction with focus on the role of the nitrogen atoms in the pyrimidine/ pyridyl moiety, the structure of the Zn-alkoxides in solution by NMR spectroscopic studies and *in-situ* IR kinetic studies using pyridyl-3-carbaldehyde as surrogate, ('Trojan-Horse' substrate). An alternative mechanism is proposed, considering a 'cube escape' model. Such cube-type structures were also proposed by Noyori and co-workers[6a] in the enantioselective addition of dialkylzincs to aldehydes promoted by chiral β-amino alcohols, i.e. (-)-3-*exo*-(dimethyl-amino)isoborneol (DAIB) and has been discussed by Brown and co-workers in the context of the Soai reaction as potential tetrameric structure of the Zn-alkoxides.[25]

Furthermore, the Soai reaction shows some peculiarities that are well documented, but still unexplained such as (a) an unusual inverse temperature dependence on the reaction kinetics, *i.e.* the maximum reaction rate increases significantly as the reaction temperature is decreased,[41] and (b) a prolonged induction period, which are not yet rationalized by properties of potential catalyst structures or corresponding kinetic models.

Here we seek to investigate the open mysteries of Soai's asymmetric autocatalysis.

First, we performed reaction kinetic investigations using multiplexing HPLC[42] in the flow-injection mode[43] (Chiralpak IB, mobile phase *n*-hexane/THF 55:45, 1.2 mL/min), which provides temporal resolution of the stereoisomers formed (Figure 1 in the Supplementary Information). Reaction progress was observed injection of sample pulses with a time interval of 2.1 min from the reaction mixture onto the chiral separation column (Figure 1a and b). We systematically varied the concentrations of the reactants and additives of the Soai reaction (2-(*tert*-butylacetylene-1-yl)pyrimidyl-5-carbaldehyde **4**: 10.6 – 41 mM, ((*R*)-2-(*tert*-butylacetylene-1-yl)pyrimidyl-5-(*iso*-butan-1-ol) **(*R*)-1** (*ee* > 99.9%): 0.266 – 4 mM; $i\text{Pr}_2\text{Zn}$: 30 – 130 mM (Figure 1b and Figures 6-23 in the Supplementary Information).

Kinetic analysis of these data gives a reaction order of 1.9 in [**4**], an order of 1 in [**1**], and an order of 0 in [$i\text{Pr}_2\text{Zn}$] (Figures 24-26 in the Supplementary Information), confirming previous studies.[41].

$$\frac{d[\mathbf{1}]}{dt} = k\,[\mathbf{4}]^{1.9}[\mathbf{1}]^{1}[i\text{Pr}_2\text{Zn}]^{0} \qquad \text{(Eq. 1)}$$

Surprisingly, when we performed the HPLC separation of the reaction mixture using isopropanol instead of THF in the mobile phase we observed the enantiomers of another compound connected by plateau formation with **4**. We identified these peaks as the isopropyl hemiacetals **(*R*)-5$_{iPr}$** or **(*S*)-5$_{iPr}$** (Figure 2 a), *i.e.* in the case of chiral alcohols diastereomeric hemiacetals are expected (*vide infra*).

Remarkably, these hemiacetals **5$_{iPr}$** are subject to a dynamic interconversion, which we investigated by temperature-dependent enantioselective dynamic HPLC (DHPLC)[44,45] (Figure 2 b and Figures 28-35 in the Supplementary Information).

The thermodynamic parameters of the formation of the hemiacetal **5$_{iPr}$** were determined by linear regression of the thermodynamic Gibbs free energies Δ*G*(*T*), obtained from the

10.1002/chem.202003260

equilibrium constants K, *vs.* the temperatures T (correlation coefficient $r = 0.9949$) to be $\Delta G^0 = 3$ kJ/ mol, $\Delta H^0 = -15.6$ kJ/ mol and $\Delta S^0 = -62.5$ J/(K·mol) (Figure 36 in the Supplementary Information).

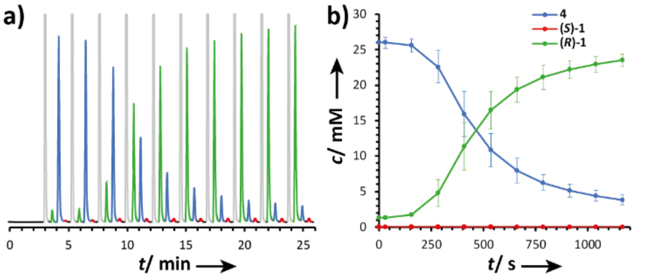

Figure 1. a) Reaction progress analysis by flow-injection analysis using enantioselective HPLC to separate the reactand **4** and product enantiomers **(*R*)-1** (green) and **(*S*)-1** (red). Reaction conditions: 26.0 mM 2-(*tert*-butylacetylene-1-yl)pyrimidyl-5-carbaldehyde **4**, 1.3 mM (*R*)-2-(*tert*-butylacetylene-1-yl) pyrimidyl-5-(*iso*-butan-1-ol) **(*R*)-1** (ee > 99.9%) and 40 mM *i*Pr_2Zn in toluene (grey) at 20°C. Separation conditions: Chiralpak IB column (25 cm, I.D. 4.6 mm, particle size 5 µm), *n*-hexane/THF 55:45 (v/v), 1.2 mL/min. b) Concentration of **(*R*)-1, (*S*)-1** and **4** *vs.* time *t*.

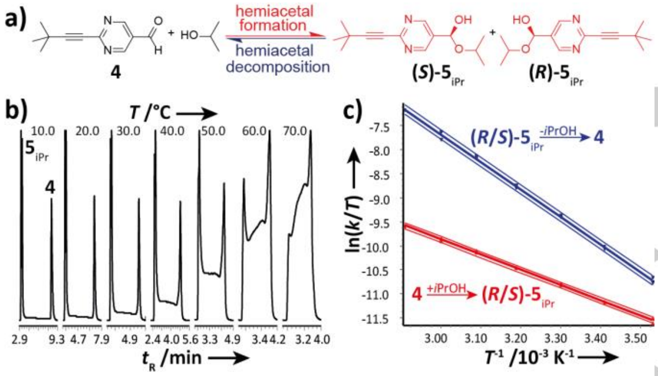

Figure 2. a) Hemiacetal formation of 4 in presence of *i*-propanol. b) Temperature-dependent enantioselective DHPLC measurements of the formation of the hemiacetal $\mathbf{5}_{iPr}$ with isopropanol (Chiralpak IC-3 (15 cm, I.D. 4.6 mm, particle size 3 µm), *n*-hexane/isopropanol 60:40 (v/v), 1.0 mL/min. c) Eyring plot for the determination of the activation parameters $\Delta H^{\ddagger}$ and $\Delta S^{\ddagger}$ of the hemiacetal formation (red data points) and the hemiacetal decomposition (blue data points) obtained from the DHPLC experiment. The upper and lower curves represent the error bands (21 data points each) of the linear regression with a level of confidence of 95%.

The activation enthalpies $\Delta H^{\ddagger}$ for the hemiacetal $\mathbf{5}_{iPr}$ formation and decomposition were obtained via the slope and the activation entropies $\Delta S^{\ddagger}$ via the intercept of the Eyring plots (ln(k/T) *vs.* 1/*T*) (Figure 2c). Deviations of the activation parameters $\Delta H^{\ddagger}$ and $\Delta S^{\ddagger}$ have been calculated by error band analysis of the linear regression with a level of confidence of 95%. The activation parameters of the hemiacetal $\mathbf{5}_{iPr}$ formation are $\Delta H^{\ddagger} = 26.3 \pm 0.2$ kJ/mol and $\Delta S^{\ddagger} = -195 \pm 34$ J/(K·mol) ($r = 0.9990$, residual deviation $s_y = 0.0306$) and the hemiacetal $\mathbf{5}_{iPr}$ decomposition are $\Delta H^{\ddagger} = 47.7 \pm 0.2$ kJ/mol and $\Delta S^{\ddagger} = -112 \pm 1$ J/(K·mol) ($r = 0.9994$, $s_y = 0.0630$). The formation of hemiacetal $\mathbf{5}_{iPr}$ from **4** is endergonic, however this is a highly dynamic process and interestingly, the kinetic parameters $k_1(293\text{ K}) = 4.1 \cdot 10^{-3}$ (mol·s)$^{-1}$ and $k_{-1}(293\text{ K}) = 1.3 \cdot 10^{-2}$ s^{-1}). Hemiacetals, formed from the pyrimidine-5-carbaldehyde and its corresponding alcohol can function as a transient chiral ligand to activate the dialkylzinc reagent, very similar to the β-dialkylaminoalcohols in Noyori's DAIB catalysis[6a] or Blackmond's hydroxy ethers.[19] The in-situ formation of a transient catalyst by reaction or interaction of molecules participating in the reaction is a fundamental mechanism leading immediately to autocatalysis and amplification. Similar mechanisms are well known in substrate activated enzyme catalysis to regulate biochemical reaction networks and in artificial systems.[46] Furthermore, the thermodynamic data indicate that the formation of the hemiacetal is favored at lower temperature and if it is involved in the autocatalytic cycle, it correlates with the observation that the Soai reaction is accelerated at lower temperature. Moreover, the measured reaction kinetics of the formation of the hemiacetals agrees with the observed induction period of the Soai reaction.

^{1}H NMR spectroscopic studies in CD_3OD reveal that the electron-deficient pyrimidine moiety of **4** and the unsubstituted pyrimidyl-5-carbaldehyde $\mathbf{4_H}$ promote the formation of deuterated methyl hemiacetals (characteristic hemiacetal proton at $\delta = 5.7$ ppm; cf. Figures 39 and 42 in the Supplementary Information) in 95% yield at room temperature, while for comparison benzaldehyde yields only 9% (Table 4 in the Supplementary Information). Temperature dependent measurements confirm the trend that the hemiacetal formation is favored at lower temperature (Figures 40 and 41 in the Supplementary Information). This formation of hemiacetals is also observed in toluene, the solvent used in the Soai reaction: Reaction of **4** and $\mathbf{4_H}$ with *rac*-2-methyl-1-phenylpropan-1-ol in [D_8]toluene give diastereomeric hemiacetals in 11% and 9% yield, respectively. More important, the diastereomeric ratio of 1:2.6 for the unsubstituted pyrimidine hemiacetal improves to 1:5.2 for the 2-(*tert*-butylacetylene-1-yl substituted pyrimidine hemiacetal (HSQC spectra depicted in in Figures 43 and 44 in the Supplementary Information). In this context, it is important to note that the formation of stereolabile hemiacetals offers the conceptual mechanism of minor enantiomer recycling[47] leading to the amplification of the major enantiomer/ diastereoisomer. In the next step, we investigated the Soai reaction by *in-situ* high-resolution mass spectrometric experiments. In these experiments there is no separation column involved to avoid quenching of the reaction intermediates. We monitored the course of the Soai reaction under inert conditions (anhydrous toluene, argon atmosphere) by feeding the reacting reaction mixture continuously (10 µL/ min) but pulsed (time interval of 30 s) via a 5 µL sample loop of a 6-port valve (anhydrous toluene as eluent, flow rate 200 µL/ min) into a high-resolution Orbitrap mass spectrometer (Figure 45 in the Supplementary Information) using atmospheric pressure chemical ionization (APCI) under mild ionization conditions ($T = 150$°C, N_2).

To identify all intermediates and transient intermediates during the Soai reaction, all pulsed injections were summed up over the complete reaction progress and the mass range between *m*/*z* 180 and 800 in a first step (Figure 3a; Figures 46-49 in the Supplementary Information). This mass spectrum shows the complexity of intermediates formed in the Soai reaction. We identified (cf. Figure 3b) the alcohol **1a** and its fragment **1b**, the monomeric Zn-alkoxides **2a** and **2b**, the dimeric Zn-alkoxides **3a** and **3b** (different charge states), pyrimidine-5-carbaldehyde **4**, the

10.1002/chem.202003260

Zn-complex of the hemiacetalate **5a**, the hemiacetal fragments **5b** and **5c**, a hydroxylated structure **5d**, which is probably formed by the ionization process, hemiacetal **5e** with *i*Pr_2Zn coordinated to it (this can be bridged or open), the hemiacetalate with coordinated toluene **5f**. Structures **7a**-**7d** are Zn-hemiacetalate complexes with another molecule or fragment of alcohol **1** coordinated, and structure **8** represents a dimeric Zn-hemiacetal complex.

The identification of the Zn complexes is facilitated by the characteristic isotope pattern of Zn (Figure 4a, right MS spectrum); for comparison, the high-resolution MS spectrum on the left side in Figure 4a shows the formation of hemiacetal **5** (*m*/*z* 421.25822) by mixing **1** and **4** in toluene. High-resolution MS spectra of the identified structures are depicted in Figures 50-63 in the Supplementary Information.

These structures were also confirmed by MS/MS measurements.

By the temporal resolution of the injection pulses in the experimental setup, the relative concentration of the transient hemiacetal intermediate **5** can be monitored in the course of the Soai reaction (Figure 4b). Interestingly, the apex of this profile coincides with the inflection point of the sigmoidal kinetic profile of the Soai reaction (Figure 4b, top), which suggests, that the transient Zn-hemiacetalate **5** is slowly built up during the induction period, is then amplified in the autocatalytic cycle and finally depleted.

The coordination of *i*Pr_2Zn to the *N* atoms of the pyrimidine rings not only activates the zinc reagent, but also favors the formation of hemiacetals by spatial arrangement (tweezer effect) and electronic effects. Interestingly, no bridged pyrimidyl alcohols **1**, pyrimidyl alkoxides **2** or pyrimidine-5-carbaldehydes **4** are observed, which can be attributed to the noncovalent nature of such complexes, which are not stable under the conditions of the APCI.

To investigate the role of the dialkylzinc reagent and the alcohol additive in the Soai reaction we performed mixing experiments. We systematically varied *i*Pr_2Zn and diethylzinc (Et_2Zn) as reagent in the reaction itself and to pre-form Zn-alkoxides **2**.

In a second set of experiments we mixed various concentrations of the additives **(*S*)-1**, **(*S*)-1$_H$** and **(*R*)-1$_H$** to study the effect on the *ee*. While in the Soai reaction of **4** with Et_2Zn only low *ee*'s are observed, the reaction with a 1:1 mixture of *i*Pr_2Zn and Et_2Zn/ **(*S*)-1** gives *ee*'s of 68% and 63% for **(*S*)-1** and **(*S*)-1$_{Et}$**, respectively (Scheme 2a).

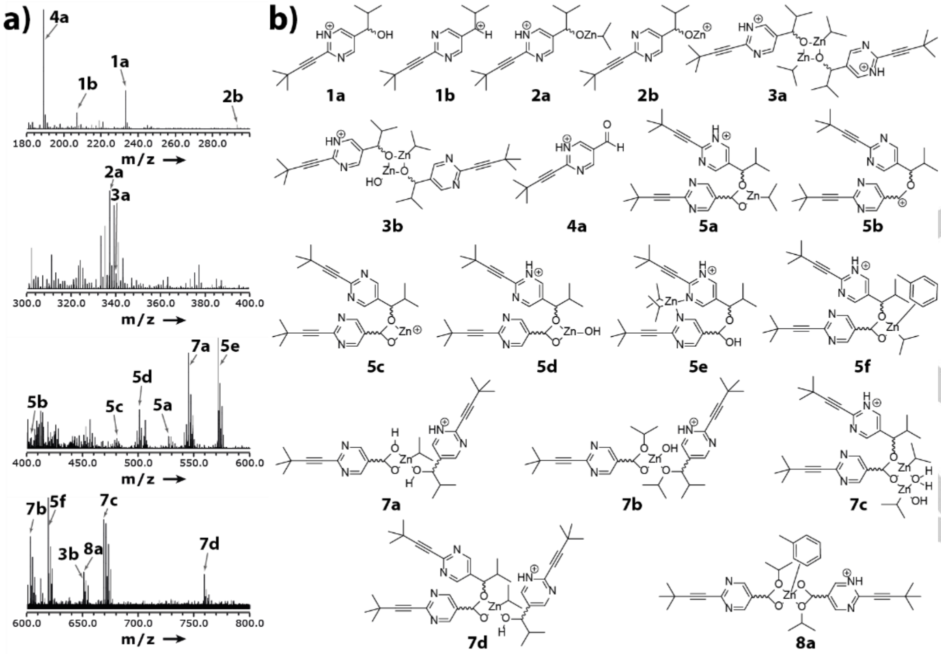

Figure 3. Identification of intermediates and transient intermediates of the Soai reaction by *in-situ* high-resolution mass spectrometry. a) Summarized mass spectra and assigned peaks covering *m*/*z* 180 – 800. b) Structures identified by high-resolution MS.

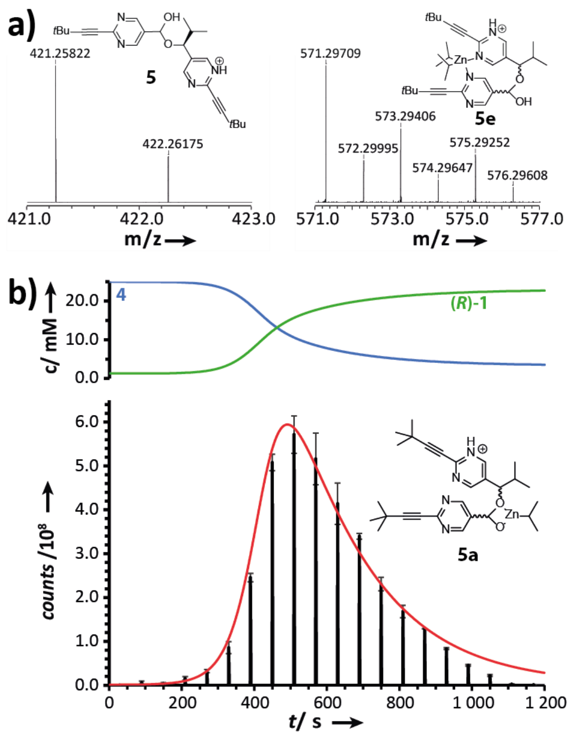

Figure 4. Investigation of the Soai reaction by *in-situ* high-resolution mass spectrometry. a) High-resolution mass spectrum of the hemiacetal **5** (left) and transient hemiacetal structure **5c** (right) obtained by in-situ MS reaction monitoring of the Soai reaction. b) Monitoring of the ion counts (bottom) of **5a** (*m*/*z* 527.234115) and **5e** (*m*/*z* 571.297085) *vs.* time during the Soai reaction (top). Reaction conditions: 25.0 mM **4**, 1.25 mM **(*R*)-1** (ee > 99.9%) and 50 mM *i*Pr_2Zn in toluene at 20°C.

10.1002/chem.202003260
WILEY-VCH

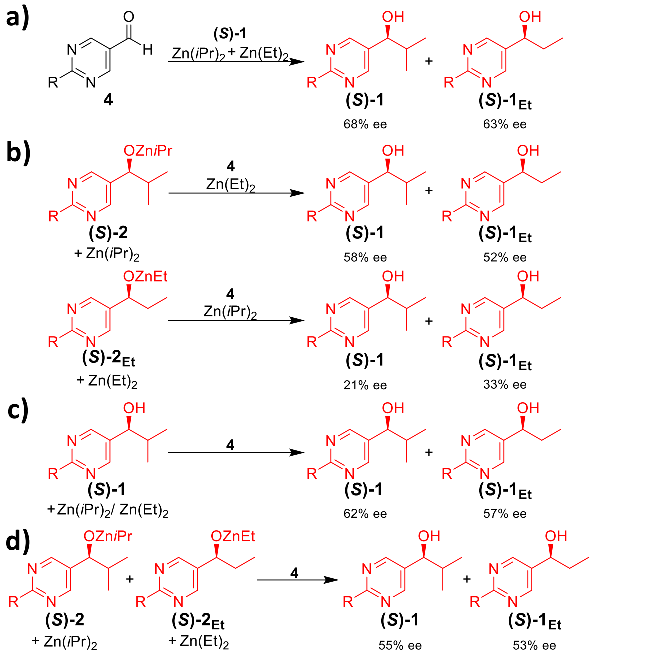

Scheme 2. Systematic variation of *i*Pr_2Zn, Et_2Zn and the additives **1** or **2**. R = –C≡C–$C(CH_3)_3$.

If the reaction is started with pre-formed **(*S*)-2** or **(*S*)-2$_{Et}$**, higher *ee*'s are observed for the isopropyl substituted alkoxide **(*S*)-2** compared to the ethyl substituted alkoxide **(*S*)-2$_{Et}$** (Scheme 2b). If *i*Pr_2Zn, Et_2Zn and **(*S*)-1** are pre-mixed, the selectivity of the isopropyl substituted alkoxide **(*S*)-2** dominates and gives higher *ee* values (Scheme 2c). This is also observed for the competitive reaction using **(*S*)-2** and **(*S*)-2$_{Et}$** simultaneously (Scheme 2d). These experiments show that the catalyst formed in the induction period strongly depends on the starting conditions and remains catalytically active and selective throughout the Soai reaction.

Table 1. Variation of the additive composition in the Soai reaction.

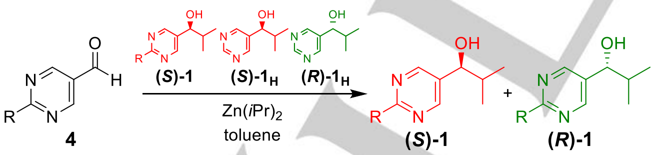

Entry	**(*S*)-1** mol%	**(*S*)-1$_H$** mol%	**(*R*)-1$_H$** mol%	% *ee*
1	5.00	-	-	95 (*S*)
2	-	5.00	-	47 (*S*)
3	3.75	1.25	-	92 (*S*)
4	1.25	3.75	-	80 (*S*)
5	2.50	-	2.50	64 (*S*)
6	1.67	-	3.33	26 (*S*)
7	1.25	-	3.75	1.5 (*R*)
8	1.00	-	4.00	14 (*R*)
9	0.86	-	4.14	28 (*R*)

R = –C≡C–$C(CH_3)_3$

This becomes evident from the mixing experiment where the concentrations of the additives **(*S*)-1**, **(*S*)-1$_H$** and **(*R*)-1$_H$** are varied. The 2-(*tert*-butylacetylene-1-yl) substituted alcohol **(*S*)-1** dominates the selectivity, resulting in high *ee* values (Table 1). Entries 4 and 5 of Table 1 show, that the catalyst formed from additive **(*S*)-1** remains catalytically active and the selectivity is controlled by the catalyst, which is better stabilized in solution. The 2-(*tert*-butylacetylene-1-yl) substituent improves the residence time and with that the turnover number. This explains also the excellent selectivities of the 2-(adamantylacetylene-1-yl)- and 2-(trimethylsilylacetylene-1-yl)-substituted pyrimidyl alcohols.[10c,37] Furthermore these mixing experiments are in good agreement with the experiments by Amedjkouh using pyrimidine alcohol **1** as chiral additive in the Soai reaction of pyridyl-3-carbaldehydes.[12e,48]

A doping experiment corroborates that the Soai reaction is catalyzed by a transient catalyst formed in the course of the reaction. For this purpose, we transferred the reaction solution of a running Soai reaction to a just started Soai reaction.

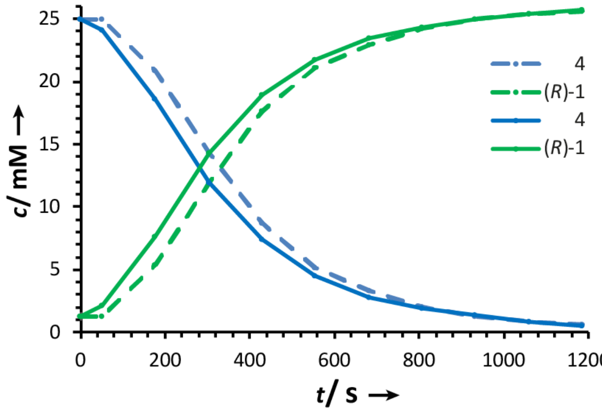

Figure 5. Reaction progress of concentrations **(*R*)-1** and **4** *vs.* time *t* of the doping experiment. The solid lines represent the Soai reaction doped with the transient catalyst solution (60 µL) formed from an immediately preceding (*t* = 218 s) Soai reaction. The dashed lines represent the reaction progress of the reference Soai reaction. Reaction conditions: 25.0 mM **4**, 1.25 mM **(*R*)-1** (ee > 99.9%) and 125 mM *i*Pr_2Zn in toluene at 20°C.

For this, four Soai reactions (25 mM 2-(*tert*-butylacetylene-1-yl)pyrimidyl-5-carbaldehyde **4**, 1.25 mM (*R*)-2-(*tert*-butylacetylene-1-yl)pyrimidyl-5-(iso-butan-1-ol) **(*R*)-1** (ee > 99.9%), 20°C, all concentrations are final concentrations after addition of the *i*Pr_2Zn solution) were prepared from the same stock solutions and distributed in 4 vials under inert reaction conditions. 2 vials were used as reference vials, one started simultaneously (1st vial) with a 2nd vial, in which the transient catalyst is formed during the reaction (for experimental details a detailed timing scheme is depicted in Figure 64 in the Supplementary Information). The Soai reactions are started by addition of *i*Pr_2Zn (125 mM final concentration). After 210 s the 3rd Soai reaction is started by addition of *i*Pr_2Zn (125 mM final concentration). 218 s after the start of the reference reaction and the Soai reaction in the 2nd vial 60 µl of the reaction solution are

10.1002/chem.202003260

transferred from the 2nd vial into the 3rd vial. The 2nd reference (4th vial) was started after the completion of reactions 1 and 2. All reactions were monitored by multiplexing HPLC in the flow-injection mode. Analysis of the kinetic data (Figure 5) shows, that the induction period is reduced in the doped experiment. Quantitative kinetic analysis confirms that the inflection point (maximum reaction rate) of the 'normal' Soai reaction (25.0 mM **4**, 1.25 mM **(*R*)-1** (*ee* > 99.9%) and 125 mM *i*Pr_2Zn in toluene at 20°C) is at 255 s with an initial reaction rate of $4.2{\cdot}10^{-3}$ mol/ s, while in the doped experiment the inflection point is at 200 s and the initial reaction rate is $1.4{\cdot}10^{-2}$ mol/ s (Figures 65-70 in the Supplementary Information). The induction period is shifted by 55 s in the doped experiment. It has to be pointed out, that adding 60 µL of a completed Soai reaction does not influence the induction period.

enantiomer directs if the autocatalytic cycle proceeds to the right autocatalytic *R*-cycle (green) or the left autocatalytic *S*-cycle (red).

Key step is the formation of the transient hemiacetal catalyst **5**, which is in a dynamic equilibrium between the zinc alkoxide **2** and aldehyde **4** forming diastereomeric complexes **(*R*,*R*)-5** or **(*R*,*S*)-5**, if **(*R*)-1** dominates, or forming diastereomeric complexes **(*S*,*S*)-5** or **(*S*,*R*)-5**, if **(*S*)-1** dominates. These structures are very similar to the zinc β-dialkylaminoalcoholate structures in Noyori's DAIB catalyst.[6a] DFT calculation at the PBE0-D3/ LACVP** level of theory as implemented in the Jaguar 10.1 quantum chemistry program package[49-55] of optimized structures of **(*R*,*R*)-5** and **(*R*,*S*)-5** indicate that the diastereomer **(*R*,*R*)-5** is favored by 6 kJ/mol (cf. Supplementary Information Figures 118 and 119). In the following only the autocatalytic *R*-cycle on the right side will be discussed, which is mirror-symmetrical to the autocatalytic *S*-cycle. In the next step of this cycle pyrimidine-5-carbaldehyde **4** and *i*Pr_2Zn are coordinated to the hemiacetal **(*R*,*R*)-5** forming adduct **(*R*,*R*)-6**. This spatial alignment of the carbaldehyde results in a transfer of the adjacent isopropyl group from the *re* side giving

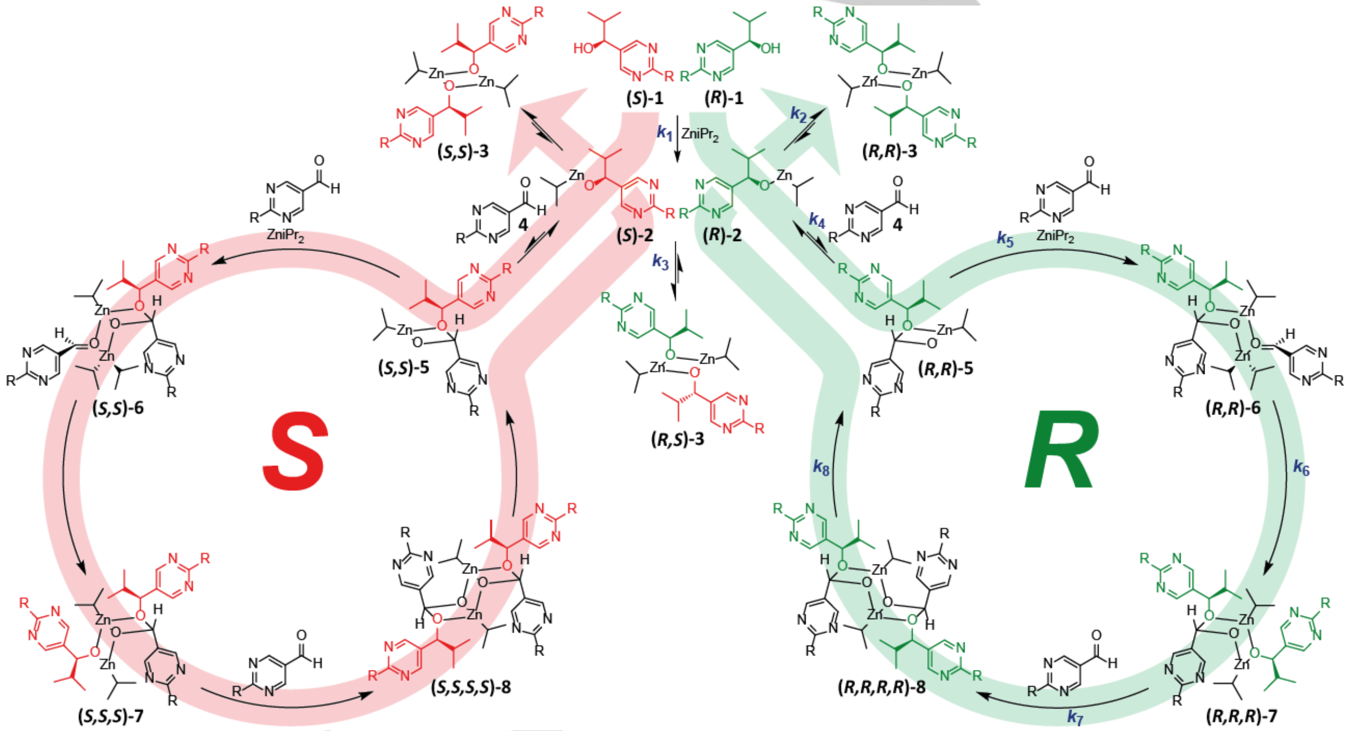

Scheme 3. Proposed mechanism of the Soai-reaction with the formation of the transient Zn-hemiacetalate catalyst **5** as key step intermediate. All structures identified by the *in-situ* high-resolution mass spectrometric experiments were considered in the mechanism. The green and red reaction arrows show the pathways to the reaction products, the dimers **3**, via Zn-hemiacetalate catalysis. R = –C≡C–$C(CH_3)_3$.

Considering all kinetic and thermodynamic data of the hemiacetal formation, the structural information obtained by the *in-situ* high-resolution mass spectrometric reaction monitoring, the transient formation of the Zn-hemiacetalate **5** during the Soai reaction, the mixing experiments and the doping experiment, we propose a reaction mechanism that can explain the high amplification of the experimentally observed enantioselectivity (Scheme 3). This mechanism starts with the formation of the isopropylzinc pyrimidyl alkoxides **2** from **(*R*)-1** and/ or **(*S*)-1**. The isopropylzinc pyrimidyl alkoxides **2** are in equilibrium with the homochiral **(*R*,*R*)-3**/ **(*S*,*S*)-3** and heterochiral **(*R*,*S*)-3** dimers. Depending on this first selection process the dominating

(*R*,*R*,*R*)-7. DFT calculations provide an energy barrier of 54 kJ/mol (cf. Supplementary Information Figures 120-123). Insertion of another molecule of the pyrimidine-5-carbaldehyde **4** leads to the dimeric hemiacetal **(*R*,*R*,*R*,*R*)-8**, which splits into two monomeric hemiacetals **(*R*,*R*)-5**, which explains the rapid sigmoidal increase in the formation of catalytically highly active **(*R*,*R*)-5** (Figure 4b) and is typical for an autocatalytic process. The dimeric hemiacetal **(*R*,*R*,*R*,*R*)-8** represents a 'super' diastereomeric complex and in combination with the dissociation into the monomeric hemiacetals **(*R*,*R*)-5**, which can dynamically control the stereocenter of the hemiacetal group, gives a natural mechanism of autocorrection. It has to be noted that **(*R*,*R*,*R*)-7**

10.1002/chem.202003260

can be also directly converted into **(*R*,*R*)-5** and **(*R*)-2** (and its corresponding dimer **(*R*,*R*)-3**).

For the evaluation of the kinetic data we developed three kinetic models (models I, II and III) with increasing complexity (Figures 71, 72 and 73 in the Supplementary Information). The minimal model (I) (Figure 71 in the Supplementary Information, 7 reaction steps) considers only a single enantiomer, the extended model (II) (Figure 72 in the Supplementary Information) considers both enantiomers, and the comprehensive model (III) (Figure 73 in the Supplementary Information) takes the epimeric hemiacetals **5** into account. It has to be pointed out that all three models result in consistent intrinsic reaction rates. The comprehensive model III consists of 26 differential equations (see Supplementary Information for details) based on the here presented mechanism (Scheme 3) was created and implemented in a software program (Soai 7).[56] This program allows to calculate kinetic reaction profiles using an adaptive Runge-Kutta routine to solve the system of differential equations with the initial experimental parameters, *i.e.* concentrations of the additives **(*R*)-1** and **(*S*)-1** (*ee*), the pyrimidin-5-carbaldehyde **4** and iPr_2Zn, the reaction time, reaction rate constants k_n (Scheme 3) and equilibrium constants K_n. This program allows to define large data sets (2.25 million kinetic profiles each) with variable ranges for the reaction rate constants k_n and equilibrium constants K_n. The calculated kinetic profiles are compared with the experimentally determined kinetic profiles of **(*R*)-1**, **(*S*)-1** and **4** (Figure 1b and Figures 6-23 in the Supplementary Information) to refine the kinetic parameters. This method was applied iteratively to all kinetic data sets (in total 81 million kinetic profiles) and thus the rate constants for the respective partial steps were determined (Figures 79-100 in the Supplementary Information). The kinetic and thermodynamic parameters are summarized in Table 2.

Table 2. Kinetic data of the Soai-reaction of aldehyde **4** with iPr_2Zn forming alcohol **1** obtained by comprehensive simulation of the proposed reaction mechanism.

n[a]	k_n[b]	K_n[c]	k_{-n}[d]
1	$1.5{\cdot}10^2 \pm 7$ M^{-1}s^{-1}		
2	$7.0{\cdot}10^2 \pm 32$ M^{-1}s^{-1}	81 ± 4 M^{-1}	8.6 ± 0.8 s^{-1}
3	$7.0{\cdot}10^2 \pm 32$ M^{-1}s^{-1}	162 ± 8 M^{-1}	4.3 ± 0.4 s^{-1}
4	$1.7{\cdot}10^{-3} \pm 1.2{\cdot}10^{-4}$ M^{-1}s^{-1}	0.136 ± 0.001 M^{-1}	$1.3{\cdot}10^{-2} \pm 1.0{\cdot}10^{-3}$ s^{-1}
5	63 ± 5 M^{-2}s^{-1}		
6	0.11 ± 0.01 s^{-1}		
7	13.2 ± 0.2 M^{-1}s^{-1}		
8	0.23 ± 0.02 s^{-1}		

[a] Reaction step as denoted in Scheme 3. [b] Forward reaction rate constants. [c] Equilibrium constants. [d] Backward reaction rate constants.

The formation of the isopropylzinc pyrimidyl alkoxides **2** is a rapid process and agrees very well with kinetic data of the reaction of alkylzinc compounds with alcohols.[57] The equilibrium between monomeric **2** and homochiral **(*R*,*R*)-3**/ **(*S*,*S*)-3** and heterochiral **(*R*,*S*)-3** is dynamic and not extremely shifted to the side of the dimers, as it is also observed in the mass spectra (Figure 3a). More interesting is the equilibrium and the kinetic parameters of the hemiacetal **5** formation, which are in excellent agreement with the kinetic parameters determined by enantioselective DHPLC (Figure 2a-c) for the formation of $\mathbf{5_{iPr}}$ (k_1(293 K) = $4.1{\cdot}10^{-3}$ (mol·s)$^{-1}$ and k_{-1}(293 K) = $1.3{\cdot}10^{-2}$ s^{-1}) and equilibria of the derivatives by ^{1}H NMR spectroscopy. In the autocatalytic cycle the rate determining step is the transfer of the isopropyl group, while the other steps are energetically balanced.

The proposed mechanism and the kinetic model allow not only to predict kinetic reaction profiles of the conversion of the pyrimidine-5-carbaldehyde **4** into the reaction product **1** of the Soai reaction, but even more important the precise prediction of the nonlinear amplification of the *ee* and the induction period in dependence on the *ee*. When starting with an *ee* of 1% in **1** (2 mmol/ L), 9.25% *ee* in the 1st step, 59.4% *ee* in the 2nd step, 94.6% *ee* in the 3rd step, 99.4% *ee* in the 4th step and 99.9% *ee* in the 5th step are obtained (Figures 101-105 of the Supplementary Information). A systematic variation of the initial ee_0 of **1** and the corresponding final product *ee* is plotted in Figure 6a (the corresponding *ee* simulations are plotted in Figures 106-115 in the Supplementary Information). Interestingly, if the reaction is performed under conditions, where the formed product with amplifying *ee* propagates through a reaction mixture, *i.e.* by diffusion or starting with seeding on a chiral or enantiomorph surface, extraordinary *ee* amplifications can be predicted, jumping immediately from $1{\cdot}10^{-5}$% to 55% and finally >99.9% (Figure 6a; red line). Experimental investigations of reactions with variation of the starting ee of the alcohol additive and concentrations were compared with the prediction of ee values by simulation with the program Soai 7, giving an excellent correlation between experiment and simulation (see Supplementary Information Table 5 and Figure 117).

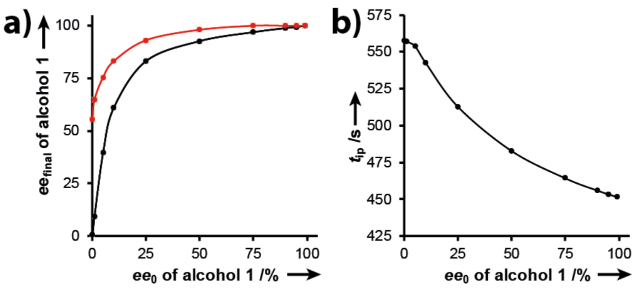

Figure 6. Enantiomeric excess and time of the inflection point in dependence on the initial ee of the added pyrimidine alcohol **1** predicted by the mechanistic model and reaction rate constants obtained by comprehensive analysis of the kinetic data. Simulations were obtained by calculations with Soai 7. a) Amplification of the *ee* (final *ee* vs. initial *ee* of the alcohol **1**). The black line represents a homogeneous and stirred reaction mixture, the red line represents a Soai reaction slowly propagating through a reaction mixture. b) Shift of the inflection point t_{ip} in dependence on the initial *ee* of **1**. Starting concentrations used for simulation: 25.0 mM **4**, 2 mM **1** (ratio of **(*R*)-1** and **(*S*)-1** depending on the corresponding *ee*) and 50 mM iPr_2Zn.

10.1002/chem.202003260

WILEY-VCH

Furthermore, the simulations correctly predict the prolonged induction period, which is caused by the slow hemiacetal formation, and the time of the inflection point t_{ip} in dependence on the initial *ee* of the pyrimidine alcohol **1** (Figure 6b).

In summary, the results of the high-resolution mass spectrometric measurements and the comprehensive kinetic analyses suggest the formation of a transient Zn-hemiacetalate complex, which is catalytically active in the Soai reaction. This intermediate can establish the here proposed autocatalytic cycle and the extraordinary amplification of the enantiomeric excess. This is supported by mass spectrometric profiling of the transient hemiacetal intermediate and by doping experiments, which demonstrate that the Soai reaction can be accelerated by adding the *in-situ* formed catalyst. Kinetic and thermodynamic data of the highly dynamic formation and decomposition of the hemiacetal explain the unusual inverse temperature dependence on the reaction kinetics, the induction period and time shift of the inflection point. Furthermore, the results suggest that the formation of the transient diastereomeric Zn-hemiacetalates amplify any initial imbalance of the formed product enantiomers, which is interestingly always given for an odd number of formed molecules. These results give a new guidance to structures envisioning potential processes leading to symmetry breaking.

Acknowledgements

We acknowledge financial support from the European Research Council ERC under Grant Agreements No. StG 258740, the Ludwig-Maximilians-University Munich, the Max-Planck-Society (Max-Planck-Fellow Research Group Origins of Life) and the Deutsche Forschungsgemeinschaft DFG (INST 86/1807-1 FUGG).

Keywords: autocatalysis • hemiacetal • kinetic analysis • mass spectrometry • Soai reaction

[1] a) J. -M. Lehn, *Angew. Chem. Int. Ed.* **2013**, *52*, 2836-2850; *Angew. Chem.* **2013**, *125*, 2906-2921; b) J.-M. Lehn, *Angew. Chem. Int. Ed.* **2015**, *54*, 3276-3289; *Angew. Chem.* **2015**, *127*, 3326-3340.
[2] D. G. Blackmond, *Chem. Rev.* **2020**, *120*, in press.
[3] a) I. Weissbuch, L. Addadi, Z. Berkovitch-Yellin, E. Gati, M. Lahav, L. Leiserowitz, *Nature* **1984**, *310*, 161-164; b) D. K. Kondepudi, R. J. Kaufman, N. Singh, *Science* **1990**, *250*, 975-976; c) B. L. Feringa, R. A. van Delden, *Angew. Chem. Int. Ed.* **1999**, *38*, 3418-3438; d) H. Zepik, E. Shavit, M. Tang, T. R. Jensen, K. Kjaer, G. Bolbach, L. Leiserowitz, I. Weissbuch, M. Lahav, *Science* **2002**, *295*, 1266; e) K. Mikami, M. Yamanaka, *Chem. Rev.* **2003**, *103*, 3369-3400; f) D. G. Blackmond, *PNAS* **2004**, *101*, 5732-5736; g) R. R. E. Steendam, M. C. T. Brouwer, E. M. E. Huijs, M. W. Kulka, H. Meekes, W. J. P. V. Enckevort, J. Raap, F. P. J. T. Rutjes, E. Vlieg, *Chem. Eur. J.* **2014**, *20*, 13527-13530; h) S. Olsson, P. M. Björemark, T. Kokoli, J. Sundberg, A. Lennartson, C. J. Mckenzie, M. Håkansson, *Chem. Eur. J.* **2015**, *21*, 5211-5219; i) J. M. Ribo, J. Crusats, Z. El-Hachemi, A. Moyano, D. Hochberg, *Chem. Sci.* **2017**, *8*, 763-769.
[4] a) D. Guillaneux, S. -H. Zhao, O. Samuel, D. Rainford, H. B. Kagan, *J. Am. Chem. Soc.* **1994**, *116*, 9430-9439; b) C. Girard, H. B. Kagan, *Angew. Chem. Int. Ed.* **1998**, *37*, 2922-2959; c) M. Klussmann, H. Iwamura, S. P. Mathew, D. H. Wells, U. Pandya, A. Armstrong, D. G. Blackmond, *Nature* **2006**, *441*, 621-623; d) T. Satyanarayana, S. Abraham, H. B. Kagan, *Angew. Chem. Int. Ed.* **2009**, *48*, 456-494; *Angew. Chem.* **2009**, *121*, 464-503; e) D. G. Blackmond, *Tetrahedron: Asymmetry* **2010**, *21*, 1630-1634; f) S. B. Tsogoeva, *Chem. Commun.* **2010**, *46*, 7662-7669.
[5] C. Puchot, O. Samuel, E. Duiiach, S. Zhao, C. Agami, H. B. Kagan, *J. Am. Chem. Soc.* **1986**, *108*, 2353-2357.
[6] a) M. Kitamura, S. Okada, S. Suga, R. Noyori, *J. Am. Chem. Soc.* **1989**, *111*, 4028-4036; b) R. Noyori, M. Kitamura, *Angew. Chem. Int. Ed.* **1991**, *30*, 49-69.
[7] K. Soai, S. Niwa, *Chem. Rev.* **1992**, *92*, 833-856.
[8] F. C. Frank, *Biochimica Biophys. Acta* **1953**, *11*, 459-463.
[9] M. E. Noble-Terán, T. Buhse, J. -M. Cruz, C. Coudret, J. -C. Micheau, *ChemCatChem* **2016**, *8*, 1836-1845.
[10] a) K. Soai, T. Shibata, H. Morioka, K. Choji, *Nature* **1995**, *378*, 767-768; b) K. Soai, T. Shibata, *J. Synth. Org. Chem., Jpn.* **1997**, *55*, 994-1005; c) T. Shibata, S. Yonekubo, K. Soai, *Angew. Chem. Int. Ed.* **1999**, *38*, 659-661; *Angew. Chem.* **1999**, *111*, 746-748; d) K. Soai, T. Shibata, I. Sato, *Acc. Chem. Res.* **2000**, *33*, 382-390.
[11] Reviews: a) K. Soai, T. Kawasaki, *Chirality* **2006**, *18*, 469-478; b) K. Soai, T. Kawasaki, *Topics in Current Chemistry* **2008**, *284*, 1-33; c) T. Gehring, M. Busch, M. Schlageter, D. Weingand, *Chirality* **2010**, *22*, E173-E182.
[12] a) K. Soai, S. Niwa, H. Hori, *J. Chem. Soc., Chem. Commun.* **1990**, 982-983; b) T. Shibata, K. Choji, T. Hayase, Y. Aizu, K. Soai, *Chem. Commun.* **1996**, 1235-1236; c) T. Shibata, K. Choji, T. Hayase, Y. Aizu, K. Soai, *Chem. Commun.* **1996**, 1235-1236; d) K. Soai, T. Sato, *Chirality* **2002**, *14*, 548-554; e) C. Romagnoli, B. Sieng, M. Amedjkouh, *Eur. J. Org. Chem.* **2015**, *2015*, 4087-4092.
[13] a) D. A. Singleton, L. K. Vo, *J. Am. Chem. Soc.* **2002**, *124*, 10010-10011; b) D. A. Singleton, L. K. Vo, *Org. Lett.* **2003**, *5*, 4337-4339.
[14] I. Sato, H. Urabe, S. Ishiguro, T. Shibata, K. Soai, *Angew. Chem. Int. Ed.* **2003**, *42*, 315-317.
[15] a) I. Sato, D. Omiya, T. Saito, K. Soai, *J. Am. Chem. Soc.* **2000**, *122*, 11739-11740; b) T. Kawasaki, M. Shimizu, D. Nishiyama, M. Ito, H. Ozawa, K. Soai, *Chem. Commun.* **2009**, 4396-4398; c) T. Kawasaki, H. Ozawa, M. Ito, K. Soai, *Chem. Lett.* **2011**, *40*, 320-321.
[16] T. Kawasaki, Y. Matsumura, T. Tsutsumi, K. Suzuki, M. Ito, K. Soai, *Science* **2009**, *324*, 492-495.
[17] A. Matsumoto, H. Ozaki, S. Harada, K. Tada, T. Ayugase, H. Ozawa, T. Kawasaki, K. Soai, *Angew. Chem. Int. Ed.* **2016**, *55*, 15246-15249.
[18] a) T. Kawasaki, Y. Okano, E. Suzuki, S. Takano, S. Oji, K. Soai, *Angew. Chem. Int. Ed.* **2011**, *50*, 8131-8133; *Angew. Chem.* **2011**, *123*, 8281-8283; b) A. Matsumoto, S. Oji, S. Takano, K. Tada, T. Kawasaki, K. Soai, *Org. Biomol. Chem.* **2013**, *11*, 2928-2931.
[19] N. A. Hawbaker, D. G. Blackmond, *ACS Cent. Sci.* **2018**, *4*, 776-780.
[20] T. Kawasaki, H. Tanaka, T. Tsutsumi, T. Kasahara, I. Sato, K. Soai, *J. Am. Chem. Soc.* **2006**, *128*, 6032-6033.
[21] a) I. Sato, R. Sugie, Y. Matsueda, Y. Furumura, K. Soai, *Angew. Chem. Int. Ed.* **2004**, *43*, 4490-4492; b) T. Kawasaki, M. Sato, S. Ishiguro, T. Saito, Y. Morishita, I. Sato, H. Nishino, Y. Inoue, K. Soai, *J. Am. Chem. Soc.* **2005**, *127*, 3274-3275.
[22] a) K. Soai, S. Osanai, K. Kadowaki, S. Yonekubo, T. Shibata, I. Sato, *J. Am. Chem. Soc.* **1999**, *121*, 11235-11236; b) I. Sato, K. Kadowaki, K. Soai, *Angew. Chem. Int. Ed.* **2000**, *39*, 1510-1512; *Angew. Chem.* **2000**, *112*, 1570-1572; c) T. Kawasaki, K. Jo, H. Igarashi, I. Sato, M. Nagano, H. Koshima, K. Soai, *Angew. Chem. Int. Ed.* **2005**, *44*, 2774-2777; *Angew. Chem.* **2005**, *117*, 2834-2837; d) T. Kawasaki, K. Suzuki, M. Shimizu, K. Ishikawa, K. Soai, *Chirality* **2006**, *18*, 479-482; e) T. Kawasaki, K. Suzuki, Y. Hakoda, K. Soai, *Angew. Chem. Int. Ed.* **2008**, *47*, 496-499; f) T. Kawasaki, S. Kamimura, A. Amihara, K. Suzuki, K. Soai, *Angew. Chem. Int. Ed.* **2011**, *50*, 6796-6798; *Angew. Chem.* **2011**, *123*, 6928-6930 g) H. Shindo, Y. Shirota, K. Niki, T. Kawasaki, K. Suzuki, Y. Araki, A. Matsumoto, K. Soai, *Angew. Chem. Int. Ed.* **2013**, *52*, 9135-9138; h) H. Mineki, Y. Kaimori, T. Kawasaki, A. Matsumoto, K. Soai, *Tetrahedron: Asymmetry* **2013**, *24*, 1365-1367; i) T. Kawasaki, M. Uchida, Y. Kaimori, T. Sasagawa, A. Matsumoto, K. Soai, *Chem. Lett.* **2013**, *42*, 711-713; j) A. Matsumoto, T. Ide, Y. Kaimori, S. Fujiwara, K. Soai, *Chem. Lett.* **2015**, *44*, 688-690; k) A. Matsumoto, S. Takeda, S. Harada, K. Soai, *Tetrahedron: Asymmetry* **2016**, *27*, 943-946.
[23] a) F. Lutz, T. Kawasaki, K. Soai, *Tetrahedron: Asymmetry* **2006**, *17*, 486-490; b) T. Kawasaki, C. Hohberger, Y. Araki, K. Hatase, K. Beckerle, J. Okuda, K. Soai, *Chem. Commun.* **2009**, 5621-5623; c) G. A. Rance, S. A. Miners, T. W. Chamberlain, A. N. Khlobystov, *Chem. Mater.* **2013**, *557*, 10-14; d) T. Kawasaki, M. Nakaoda, Y. Takahashi, Y. Kanto, N. Kuruhara, K. Hosoi, I. Sato, A. Matsumoto, K. Soai, *Angew. Chem. Int. Ed.* **2014**, *53*, 11199-11202; *Angew. Chem.* **2014**, *53*, 11381-11384; e) C. J. Welch, K. Zawatzky, A. A. Makarov, S. Fujiwara, A. Matsumoto, K. Soai, *Org. Biomol. Chem.* **2017**, *15*, 96-101; f) A. Matsumoto, K. Yonemitsu, H. Ozaki, J. Misek, I. Stary, I. G. Stara, K. Soai, *Org. Biomol. Chem.* **2017**, *15*, 1321-1324.

[24] K. Soai, I. Sato, T. Shibata, S. Komiya, M. Hayashi, Y. Matsueda, H. Imamura, T. Hayase, H. Morioka, H. Tabira, J. Yamamoto, Y. Kowata, *Tetrahedron: Asymmetry* **2003**, *14*, 185-188.
[25] J. M. Brown, I. Gridnev, J. Klankermayer, *Topics in Current Chemistry* **2008**, *284*, 35-65.
[26] a) K. Micskei, G. Póta, L. Caglioti, G. Pályi, *J. Phys. Chem. A* **2006**, *110*, 5982-5984; b) D. G. Blackmond, O. K. Matar, *J. Phys. Chem. B* **2008**, *112*, 5098-5104; c) G. Lente, *Tetrahedron: Asymmetry* **2011**, *22*, 1595-1599; d) J. -C. Micheau, C. Coudret, J. -M. Cruz, T. Buhse, *Phys. Chem. Chem. Phys.* **2012**, *14*, 13239-13248; e) B. Barabás, C. Zucchi, M. Maioli, K. Micskei, G. Pályi, *J. Mol. Model.* **2015**, *21*, 33; f) I. D. Gridnev, A. K. Vorobiev, *ACS Catal.* **2012**, *2*, 2137-2149.
[27] I. D. Gridnev, A. K. Vorobiev, *Bull. Chem. Soc. Jpn.* **2015**, *88*, 333-340.
[28] a) J. R. Islas, D. Lavabre, J. -M. Grevy, R. H. Lamoneda, H. R. Cabrera, J. -C. Micheau, T. Buhse, *PNAS* **2005**, *102*, 13743-13748; b) J. -C. Micheau, J. -M. Cruz, C. Coudret, T. Buhse, *CHEMPHYSCHEM* **2010**, *11*, 3417-3419.
[29] J. Podlech, T. Gehring, *Angew. Chem. Int. Ed.* **2005**, *44*, 5776-5777; *Angew. Chem.* **2005**, *117*, 5922-5924.
[30] F. G. Buono, D. G. Blackmond, *J. Am. Chem. Soc.* **2003**, *125*, 8978-8979.
[31] I. D. Gridnev, J. M. Serafimov, H. Quiney, J. M. Brown, *Org. Biomol. Chem.* **2003**, *1*, 3811-3819.
[32] D. G. Blackmond, C. R. McMillan, S. Ramdeehul, A. Schorm, J. M. Brown, *J. Am. Chem. Soc.* **2001**, *123*, 10103-10104.
[33] D. G. Blackmond, *Tetrahedron: Asymmetry* **2006**, *17*, 584-589.
[34] J. Klankermayer, I. D. Gridnev, J. M. Brown, *Chem. Commun.* **2007**, 3151-3153.
[35] A. Matsumoto, T. Abe, A. Hara, T. Tobita, T. Sasagawa, T. Kawasaki, K. Soai, *Angew. Chem. Int. Ed.* **2015**, *54*, 15218-15221; *Angew. Chem.* **2015**, *127*, 15433-15436.
[36] I. D. Gridnev, J. M. Serafimov, J. M. Brown, *Angew. Chem. Int. Ed.* **2004**, *43*, 4884-4887.
[37] M. Busch, M. Schlageter, D. Weingand, T. Gehring, *Chem. Eur. J.* **2009**, *15*, 8251-8258.
[38] a) L. Schiaffino, G. Ercolani, *Angew. Chem. Int. Ed.* **2008**, *47*, 6832-6835; b) L. Schiaffino, G. Ercolani, *CHEMPHYSCHEM* **2009**, *10*, 2508-2515; c) L. Schiaffino, G. Ercolani, *Chem. Eur. J.* **2010**, *16*, 3147-3156; d) G. Ercolani, L. Schiaffino, *J. Org. Chem.* **2011**, *76*, 2619-2626.
[39] T. Gehring, M. Quaranta, B. Odell, D. G. Blackmond, J. M. Brown, *Angew. Chem. Int. Ed.* **2012**, *51*, 9539-9542.
[40] S. V. Athavale, A. Simon, K. N. Houk, S. E. Denmark, *Nature Chemistry* **2020**, *12*, 412-423.
[41] M. Quaranta, T. Gehring, B. Odell, J. M. Brown, D. G. Blackmond, *J. Am. Chem. Soc.* **2010**, *132*, 15104-15107.
[42] a) O. Trapp, *Angew. Chem. Int. Ed.* **2007**, *46*, 5609-5613; *Angew. Chem.* **2007**, *119*, 5706-5710; b) A. F. Siegle, O. Trapp, *Anal. Chem.* **2014**, *86*, 10828-10833; c) A. F. Siegle, O. Trapp, *Anal. Chem.* **2015**, *87*, 11932-11934.
[43] C. J. Welch, X. Gong, W. Schafer, E. C. Pratt, T. Brkovic, Z. Pirzada, J. F. Cuff, B. Kosjek, *Tetrahedron: Asymmetry* **2010**, *21*, 1674-1681.
[44] a) O. Trapp, G. Schoetz, V. Schurig, *Chirality* **2001**, *13*, 403-414; b) I. D'Acquarica, F. Gasparrini, M. Pierini, C. Villani, G. Zappia, *J. Sep. Sci.* **2006**, *29*, 1508-1516; c) C. Wolf, *Dynamic Stereochemistry of Chiral Compounds - Principles and Applications*, RSC Publishing, Cambridge, **2008**; d) O. Trapp, *Topics in Current Chemistry* **2013**, *341*, 231-270.
[45] a) O. Trapp, V. Schurig, *J. Am. Chem. Soc.* **2000**, *122*, 1424-1430; b) O. Trapp, *Anal. Chem.* **2006**, *78*, 189-198; c) O. Trapp, *Electrophoresis* **2006**, *27*, 534-541; d) O. Trapp, *Electrophoresis* **2006**, *27*, 2999-3006; e) F. Maier, O. Trapp, *Angew. Chem. Int. Ed.* **2012**, *51*, 2985-2988; *Angew. Chem.* **2012**, *124*, 3039-3043.
[46] a) H. Fanlo-Virgós, A. -N. R. Alba, S. Hamieh, M. Colomb-Delsuc, S. Otto, *Angew. Chem. Int. Ed.* **2014**, *53*, 11346-11350; b) C. Kremer, A. Lützen, *Chem. Eur. J.* **2013**, *19*, 6162-6196.
[47] a) E. Wingstrand, A. Laurell, L. Fransson, K. Hult, C. Moberg, *Chem. Eur. J.* **2009**, *15*, 12107-12113; b) L. Fransson, C. Moberg, *ChemCatChem* **2010**, *2*, 1523-1532; c) L. Fransson, A. Laurell, K. Widyan, E. Wingstrand, K. Hult, C. Moberg, *ChemCatChem* **2010**, *2*, 683-693; d) A. Laurell, C. Moberg, *Eur. J. Org. Chem.* **2011**, *2011*, 3980-3984; e) Y. -Q. Wen, R. Hertzberg, I. Gonzalez, C. Moberg, *Chem. Eur. J.* **2014**, *20*, 3806-3812; f) C. Moberg, *Acc. Chem. Res.* **2016**, *49*, 2736-2745.
[48] M. Funes-Maldonado, B. Sieng, M. Amedjkouh, *Eur. J. Org. Chem.* **2015**, *2015*, 4081-4086.
[49] C. Adamo, V. Barone, *Chem. Phys. Lett.* **1998**, *298*, 113-119.
[50] a) J. P. Perdew, K. Burke, M. Ernzerhof, *Phys. Rev. Lett.* **1996**, *77*, 3865-3868; b) Errata: J. P. Perdew, K. Burke, M. Ernzerhof, *Phys. Rev. Lett.* **1997**, *78*, 1396.
[51] S. Grimme, E. Antony, T. Ehrlich, E. Krieg, *J. Chem. Phys.* **2010**, *132*, 154104.
[52] P. J. Hay, I. R. Wadt, *J. Chem. Phys.* **1985**, *82*, 299-310.
[53] P. C. Hariharan, J. A. Pople, *Theoretica Chimica Acta* **1973**, *28*, 213-222.
[54] Jaguar, version 10.1, Schrodinger, Inc., New York, NY, 2018.
[55] A. D. Bochevarov, E. Harder, T. F. Hughes, J. R. Greenwood, D. A. Braden, D. M. Philipp, D. Rinaldo, M. D. Halls, J. Zhang, R. A. Friesner, *Int. J. Quantum Chem.* **2013**, *113*, 2110-2142.
[56] O. Trapp, Soai 7, compatible with Microsoft Windows 7, 8 and 10. The compiled executable program can be obtained from the author upon request.
[57] R. J. Herold, S. L. Aggarwal, V. Neff, *Can. J. Chem.* **1963**, *41*, 1368-1380.

WILEY-VCH

Entry for the Table of Contents

Research Article

In situ MS reaction profiling captures transient intermediates: *High-resolution mass spectrometric measurements reveal the formation of transient hemiacetal complexes. A mechanism is proposed based on identified transient structures, comprehensive kinetic analysis and modelling.*

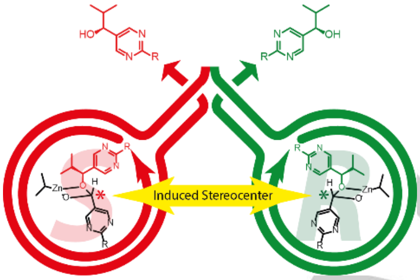

Oliver Trapp, Saskia Lamour, Frank Maier, Alexander F. Siegle, Kerstin Zawatzky, Bernd F. Straub*

Page No. – Page No.

In situ Mass Spectrometric and Kinetic Investigations of Soai's Asymmetric Autocatalysis